AD_____

Award Number: W81XWH-12-1-0328

TITLE:
Hyperpolarized 13C MR markers of renal tumor aggressiveness

PRINCIPAL INVESTIGATOR: Dr. Renuka Sriram

CONTRACTING ORGANIZATION: University of California, San Francisco

REPORT DATE: October 2013

TYPE OF REPORT: Annual

PREPARED FOR: U.S. Army Medical Research and Materiel Command
Fort Detrick, Maryland 21702-5012

REPORT DOCUMENTATION PAGE

Form Approved
OMB No. 0704-0188

1. REPORT DATE	2. REPORT TYPE	3. DATES COVERED
October 2013	Annual	15September2012–14September2013

4. TITLE AND SUBTITLE
Hyperpolarized 13C MR Markers of Renal Tumor Aggressiveness

5a. CONTRACT NUMBER

5b. GRANT NUMBER
W81XWH-12-1-0328

5c. PROGRAM ELEMENT NUMBER

6. AUTHOR(S)
Renuka Sriram
And Betty Diamond

E-Mail: Renuka.sriram@ucsf.edu,

5d. PROJECT NUMBER

5e. TASK NUMBER

5f. WORK UNIT NUMBER

7. PERFORMING ORGANIZATION NAME(S) AND ADDRESS(ES)

AND ADDRESS(ES)
University of California, San Francisco,
San Francisco, CA94103

8. PERFORMING ORGANIZATION REPORT NUMBER

9. SPONSORING / MONITORING AGENCY NAME(S) AND ADDRESS(ES)
U.S. Army Medical Research and Materiel Command
Fort Detrick, Maryland 21702-5012

10. SPONSOR/MONITOR'S ACRONYM(S)

11. SPONSOR/MONITOR'S REPORT NUMBER(S)

12. DISTRIBUTION / AVAILABILITY STATEMENT
Approved for Public Release; Distribution Unlimited

13. SUPPLEMENTARY NOTES

14. ABSTRACT
The incidence of renal cell carcinomas (RCCs) has been steadily increasing, in part due to widespread use of cross-sectional imaging. RCCs have a wide range of aggressiveness, which is currently difficult to assess noninvasively. This has resulted in overtreatment of indolent tumors, and possibly under-treatment of aggressive ones. Therefore, there is an unmet clinical need to be able to reliably distinguish renal cancer aggressiveness for optimal triage of therapies. Hyperpolarized (HP) 13C magnetic resonance spectroscopic imaging (MRSI) is a new metabolic imaging approach that is capable of interrogating specific enzymatic pathways in real time. Building on our previous work, on immoratalized cells, we aim to interrogate tumor metabolism in more clinically relevant RCC tumor models by employing patient-derived tumor tissues in conjunction with HP MRSI in this work. The patient-derived tumor models, including tissue slices maintained in a bioreactor and orthotopic mouse model, can better recapitulate the heterogeneous range of RCCs and facilitate identification of clinically relevant markers of tumor aggressiveness. During the first year, we have successfully established the *in vivo* animal model even with low grade tumors and have accomplished bioreactor *HP* experiments using live patient derived tumor tissue.

15. SUBJECT TERMS
Renal Cell Carcinoma, Hyperpolarized 13C MR, Sub-renal capsule, patient derived tissue slice cultures, bioreactor

16. SECURITY CLASSIFICATION OF:			17. LIMITATION OF ABSTRACT	18. NUMBER OF PAGES	19a. NAME OF RESPONSIBLE PERSON
a. REPORT	b. ABSTRACT	c. THIS PAGE			USAMRMC
U	U	U	UU	9	19b. TELEPHONE NUMBER *(include area code)*

Table of Contents

INTRODUCTION:

The incidence of renal cell carcinomas (RCCs) has been steadily increasing, in part due to widespread use of cross-sectional imaging[1]. RCCs have a wide range of aggressiveness, which is currently difficult to assess noninvasively. This has resulted in overtreatment of indolent tumors, and possibly under-treatment of aggressive ones. Therefore, there is an unmet clinical need to be able to reliably distinguish renal cancer aggressiveness for optimal triage of therapies. Hyperpolarized (HP) ^{13}C magnetic resonance spectroscopic imaging (MRSI) is a new metabolic imaging approach that is capable of interrogating specific enzymatic pathways in real time. We have already demonstrated in immortalized RCC cells that make more lactate (consistent with increased glycolysis) than renal proximal tubule cells, and RCC aggressiveness relates to the degree of lactate export to the extracellular space[2]. Building on this work, in this proposal, we aim to interrogate tumor metabolism in more clinically relevant RCC tumor models by employing patient-derived tumor tissues in conjunction with HP MRSI. The patient-derived tumor models, including tissue slices maintained in a bioreactor and orthotopic mouse model, can better recapitulate the heterogeneous range of RCCs and facilitate identification of clinically relevant markers of tumor aggressiveness. Specifically,

Aim 1:Identify HP 13C metabolic markers that discriminate benign renal tumors from RCCs, and low grade from high grade RCCs using human TSCs cultured in a bioreactor.

Aim 2:Identify HP 13C metabolic markers that discriminate benign renal tumors from *RCCs, and low* grade from high grade RCCs using human tumor tissues implanted under renal capsule of mice.

There has been no change in the tasks specified in Aims 1 and 2 from those proposed in the original Statement of Work, and below I describe the research that has been accomplished for each aim.

BODY:

Task 1. Approval for Animal/Human substance (Months 1-4): The animal and human substance use approval was completed within the time frame.

Development of patient-derived renal tumor tissue slice cultures (TSC): Under the guidance of Dr.Peehl, we successfully implemented a protocol to acquire renal tumor tissues from nephrectomies and to culture the slices. Specifically, 8mm cores of cancer and normal tissues were obtained from nephrectomy specimens and sliced using Krumdieck slicer. With a precision gauge micrometer, the slice thickness was maintained around 320-350 micron, which allows optimal nutrient diffusion[3]. The temporal viability of TSC was measured using LIVE/DEAD assay (n=4 each of cancer and normal renal TSCs). As seen in **Figure 1,** the TSC had maximum percentage of live cells ~24 hours post incubation. There was no significant difference in viability between cancer and normal slices. Based on these measurements, the ex vivo bioreactor experiments were performed after 16 hours of incubation for optimal viability.

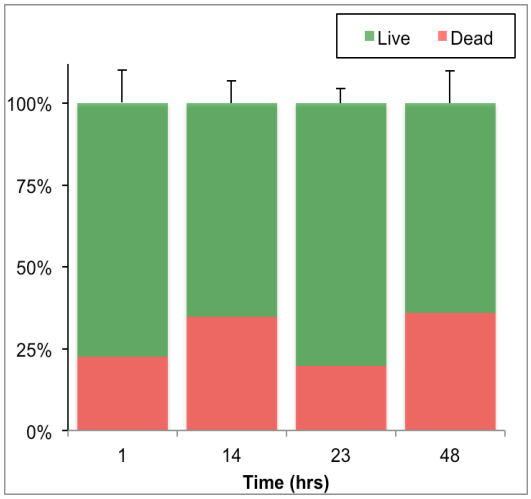

Figure 1. Measure of % live and cells over 48 hours using fluorescent dyes incubated with TSCs

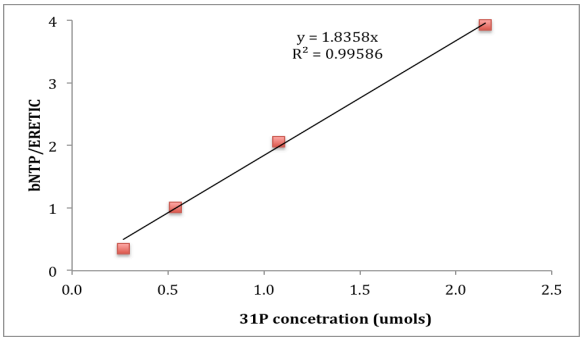

Figure 2. Calibration of the Eretic peak.

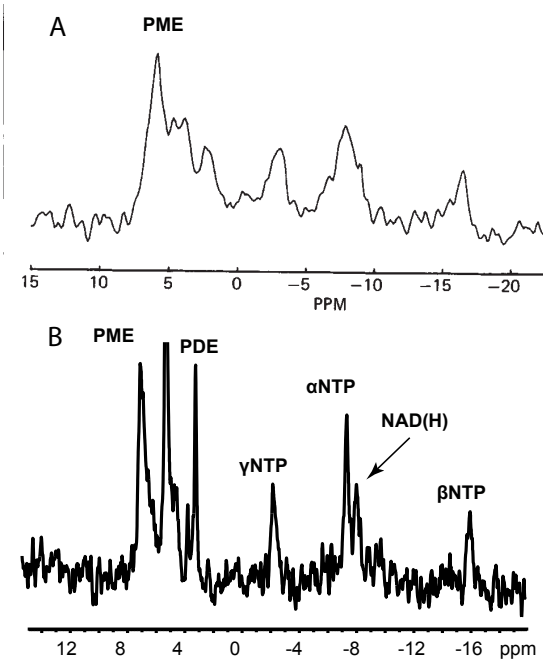

Figure 3. A)[31]P spectra from a perfused human kidney with RCC (~60g) (from Ross et al 1986). B) [31]P spectra from 4 slices of patient derived RCC TSC in the bioreactor (~60 mg).

Aim 1: Ex vivo bioreactor experiments

We first acquired phosphorous-31 ([31]P) MRS to confirm the viability of the TSC in the bioreactor by assessing the βNTP peak over time. The quantification of the βNTP peak is feasible by using an electronic reference signal (ERETIC)[4]. **Figure 2** shows the ERETIC calibration constant for ATP in the 5mm broadband probe used for acquisition. By using the slope of the correlation curve, the ratio of peak of interest to ERETIC will yield the absolute concentration. This provides an additional parameter (other than tissue wet weight) that can be employed to normalize the carbon signals across the different samples. The [31]P MR of the tissue slices showed characteristic high PME (phospho-monoesters), as seen in the literature[5] (**Figure 3)**. The spectrum also demonstrated excellent SNR and homogeneity. Four slices of RCC had mean bNTP of 36 nmols (n=4), while the normal renal tissue slices (of similar dimension) had very low bNTP levels (~11 nmols). Of note, the 5mm bioreactor used for the tissue slice studies was optimized that allows metabolic evaluation of small amount of tissue (~60mg).

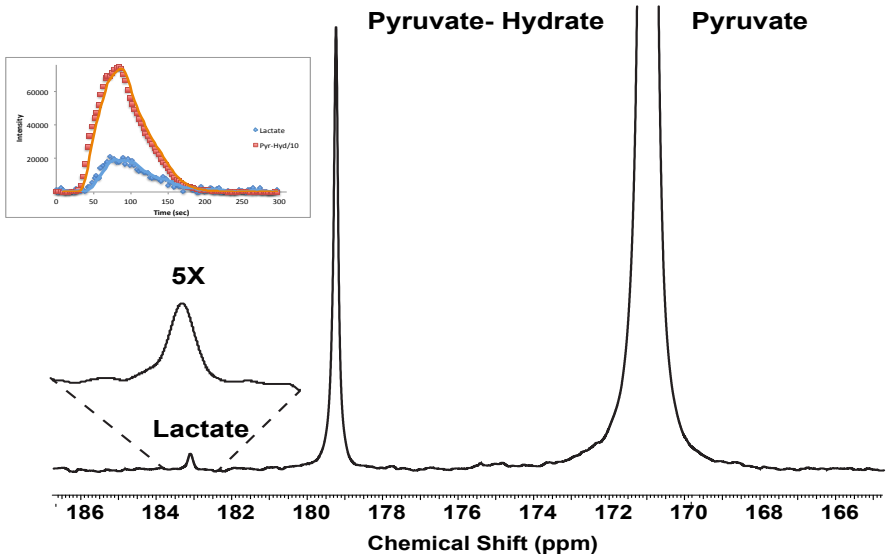

Figure 4. The hyperpolarized spectrum of 1-[13]C pyruvic acid in 4 TSCs of grade 2 clear cell RCC clearly shows the hyperpolarized signal of Lactate (enlarged 5 times). Additionally the inset shows the dynamic production of lactate in the TSCs over a period of 2 minutes

[13]C Pyruvic acid was prepared for dynamic nuclear polarization as previously reported [6], [7], and injected into the bioreactor. The MR protocol was also modified for enhanced signal acquisition. **Figure 4** shows the hyperpolarized 13C pyruvate data acquired from 4 renal tissue slices from a grade 2 renal clear cell carcinoma. [1]3C pyruvate conversion to lactate was visualized dynamically over a period of 2 minutes. In addition to lactate, we were also able to observe formation of bicarbonate and carbon-dioxide (CO_2), indicating visualization of the tricarboxylic acid (TCA) cycle metabolism, in some instances.

Figure 5. Metabolism of hyperpolarized [1,2-$^{13}C_2$] pyruvic acid of transitional cell carcinoma

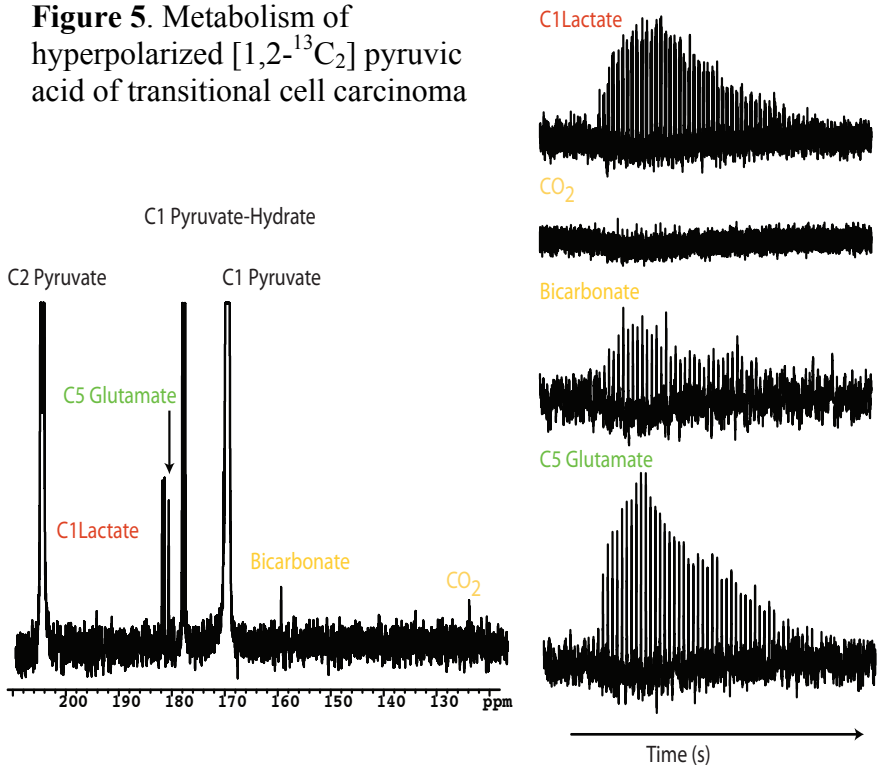

In addition to [1-^{13}C] labeled pyruvic acid, we also employed the dual labeled [1,2-$^{13}C_2$] pyruvic acid to study metabolism in the tissue slices. With this probe, we were able to observe metabolites in the TCA cycle, including glutamate, CO_2 and bicarbonate, as shown in **Figure 5**. Further optimization with this dual labeled pyruvate is in progress in addition to the other probes fructose and bicarbonate.

Kinetic modeling: We successfully implemented the 2 compartment model (**Figure 6)** to fit the flux from pyruvate to lactate using the matrix notation similar to previously published work [9,10], where T_1 represents the longitudinal relaxation rate of pyruvate and lactate (P and L) and k_{LP} is the flux from lactate to pyruvate and vice versa. IF represents the input function of the pyruvic acid bolus which was modeled based on a gamma variate function [11]. This differential equation dx/dt=Dx has a simple solution similar to the modified Bloch equation $x(t)=\exp[D(t-t_0)]x_0$. A sample of the fit to a grade 2 clear cell RCC TSC is shown in **Figure 6.** The average T1 of Pyruvate and Lactate obtained from the fit are 57±8 and 37±3 seconds (n=4). The T1 estimated for Pyruvate at 11.7T is 10 sec longer than that measured in vitro [12] while that of Lactate is close to the 32sec measured at 14T [13]. The flux to lactate was fitted to a mean value of 0.475±0.013 sec^{-1} measured in 3 normal TSCs, and the flux of pyruvate to lactate was 0.116±0.005 sec^{-1}

$$\frac{d}{dt}\begin{bmatrix} Pyr \\ Lac \end{bmatrix} = \begin{bmatrix} -1/T_{1L}-k_{PL}-0.5/f1 & k_{LP} \\ -1/T_{1L}-k_{PL}-0.5/f2 & k_{PL} \end{bmatrix} \times \begin{bmatrix} Pyr \\ Lac \end{bmatrix} + \begin{bmatrix} IF \\ 0 \end{bmatrix}$$

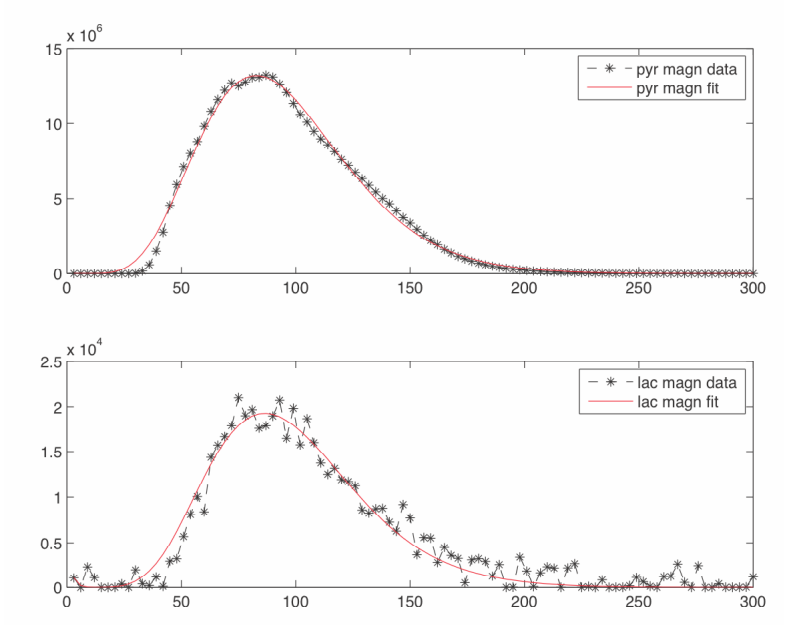

Figure 6. A) The set of differential equations for the 2 metabolites Pyruvate and Lactate in matrix notation. B) The dynamic modeling of pyruvate and C)the fit to lactate formed in the bioreactor by TSCs.

Histology: The tissue slices after the bioreactor experiment were fixed in formalin for

immunohistochemical staining (IHC) for H&E and Ki67 (indicator of proliferation). Approximately 10% of cells were proliferatiing in the cancer TSCs. Total RNA was then extracted from these TSCs and assayed for various proteins. The mean value of the various enzymes and transporters assayed are shown in Table 1 for cancer slices as a percentage to HPRT housekeeping gene. The LDHA shows a significant trend of being higher in clear cell RCC compared to the benign oncocytoma, suggesting that higher rate of glycolysis is associated with tumor aggressiveness.

Table 1:

		LDHA	LDHB	MCT1	MCT4
cc RCC (n=4)	Mean	894	1430	314	4.51
	S.E	97	195	126	1.1
Oncocytoma (n=2)	Mean	198	1050	20	1.02
	S.E	81	636	0	1.02

Aim 2: Orthotopic model of RCC using patient-derived tumor tissue slices

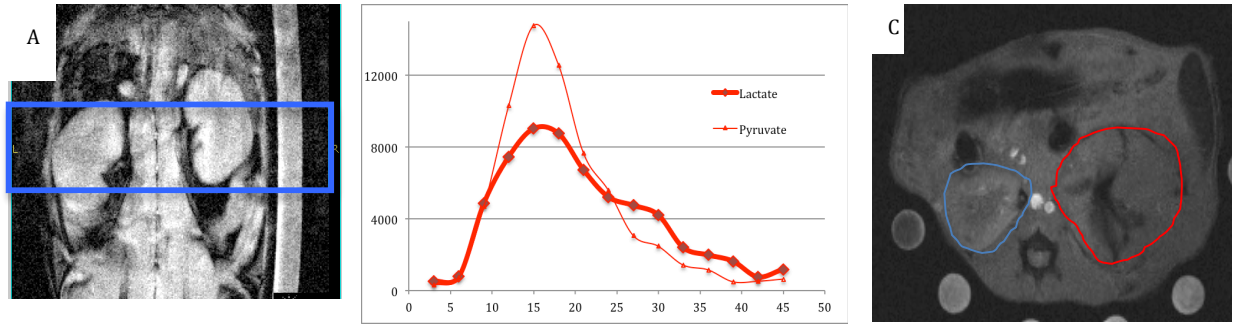

Figure 7. A) T1-weighted image of normal mice with the blue box representing the slab from which the carbon-13 data is acquired. B) Dynamic change in hyperpolarized pyruvate and lactate signals and C) aggressive ccRCC implanted in the immune compromised mice. The blue region indicates the normal right kidney of the mice and the kidney demarcated in red represents the left kidney that has been completely infiltrated by the human TSC graft.

The Rag2-IL2g receptor knockout animals were used for developing the sub-renal capsule. The TSCs grafts were slow growing, anywhere from 3-6 months depending on the tissue type, which was compatible with what was reported in the literature [15]. Multi-parametric proton imaging including T1 and T2 weighted, diffusion weighted with apparent diffusion constant maps (ADC), as well as contrast enhanced imaging, was obtained in these animals. The observed ADC values of the tumor TSCs were 1.23e^{-3} mm^2/sec, and were similar to that reported for RCCs in patients [16]. The contrast enhanced images confirmed vascularization of the TSCs under the mouse renal capsule. We additionally refined the imaging protocol for dynamic acquisition of hyperpolarized carbon-13 data. The spectral and spatially selective pulse [17], [18], [19] with up to 5 frequencies (metabolites) were optimized for high field imaging. The flip angle of the pyruvic acid was optimized using a variable flip scheme [20] while the lactate was fixed to 90 degree. In initial studies, the carbon-13 data was acquired through a slab of

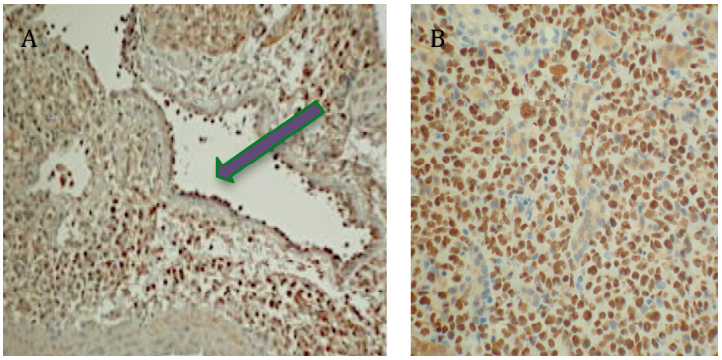

Figure 8. A) CD31 staining shows presence of human vasculature (arrow) b) Ku70 staining confirms the cells are of human origin

8mm positioned through the left kidney (in which the slice was implanted) and the dynamic changes in both the pyruvate and lactate is shown in **Figure 7**.

IHC on the TSC grafts from the animals revealed that the positive stain of human vasculature in the tumor graft was maintained, as shown by CD31 (human vasculature) and Ku70 (human cells) staining (**Figure 8),** which suggests that the tumor graft maintained features of the human tumors**.**

KEY RESEARCH ACCOMPLISHMENTS:

- Demonstrated the feasibility of using the bioreactor platform for studying the metabolism of malignant and benign living human renal tissue slice cultures using a combination of ^{31}P MRS and hyperpolarized magnetic resonance imaging
- Established a patient-derived RCC graft in the sub renal capsule of mice and used it to study RCC metabolism. Demonstrated that this orthotopic mouse model maintained human vasculature.

REPORTABLE OUTCOMES:

- Oral Presentation: Renuka Sriram, Kayvan R Keshari, Mark Van Criekinge, John Kurhanewicz, David M Wilson, Donna M Peehl, and Zhen J Wang. "**Establishment of patient-derived models of renal cell carcinoma to study metabolism and develop relevant clinical biomarkers"** presented at International Society of Magnetic Resonance in Medicine annual meeting 2013, Salt Lake City, USA

CONCLUSION:

In the first year, we have successfully established both the *ex vivo* as well as the *in vivo* model systems of RCC to study metabolism using hyperpolarized carbon magnetic resonance. We have also implemented the flux model for the bioreactor data analysis and are well on our way to acquiring more ex vivo and in vivo data. In the following year, we hope to obtain more data and stratify the tumor lactate production based on aggressiveness as postulated.

REFERENCES:

1. Sun, M. *et al.* Age-adjusted incidence, mortality, and survival rates of stage-specific renal cell carcinoma in North America: a trend analysis. *European Urology* **59,** 135–141 (2011).
2. Keshari, K. R. *et al.* Hyperpolarized 13C-Pyruvate Magnetic Resonance Reveals Rapid Lactate Export in Metastatic Renal Cell Carcinomas. *Cancer research* **73,** 529–538 (2013).
3. Malda, J., Klein, T. J. & Upton, Z. The roles of hypoxia in the in vitro engineering of tissues. *Tissue Eng.* **13,** 2153–2162 (2007).
4. Albers, M. J. *et al.* Evaluation of the ERETIC method as an improved quantitative reference for 1H HR-MAS spectroscopy of prostate tissue. *Magn Reson Med* **61,** 525–532 (2009).
5. Ross, B., Freeman, D. & Chan, L. Contributions of nuclear magnetic resonance to renal biochemistry. *Kidney Int* **29,** 131–141 (1986).
6. Keshari, K. R. *et al.* Hyperpolarized [2-13C]-fructose: a hemiketal DNP substrate for in vivo metabolic imaging. *J Am Chem Soc* **131,** 17591–17596 (2009).
7. Wilson, D. M. *et al.* Multi-compound polarization by DNP allows simultaneous assessment of multiple enzymatic activities in vivo. *J Magn Reson* **205,** 141–147 (2010).
8. Gallagher, F. A. *et al.* Magnetic resonance imaging of pH in vivo using hyperpolarized 13C-labelled bicarbonate. *Nature* **453,** 940–943 (2008).
9. Harrison, C. *et al.* Comparison of kinetic models for analysis of pyruvate-to-lactate

exchange by hyperpolarized 13 C NMR. *NMR Biomed.* **25,** 1286–1294 (2012).
10. Spielman, D. M. *et al.* In vivo measurement of ethanol metabolism in the rat liver using magnetic resonance spectroscopy of hyperpolarized [1- 13C]pyruvate. *Magn Reson Med* **62,** 307–313 (2009).
11. Ardenkjaer-Larsen, J. H., Jóhannesson, H., Petersson, J. S. & Wolber, J. in *Methods in Molecular Biology* **771,** 655–689 (Humana Press, 2011).
12. Wilson, D. M. *et al.* Generation of hyperpolarized substrates by secondary labeling with [1,1-13C] acetic anhydride. *Proceedings of the National Academy of Sciences* **106,** 5503–5507 (2009).
13. Chen, A. P. *et al.* In vivo hyperpolarized 13C MR spectroscopic imaging with 1H decoupling. *J Magn Reson* **197,** 100–106 (2009).
14. Thong, A. E. *et al.* Tissue slice grafts of human renal cell carcinoma: An authentic preclinical model with high engraftment rate and metastatic potential. *Urologic Oncology: Seminars and Original Investigations* (2013). doi:10.1016/j.urolonc.2013.05.008
15. Grisanzio, C. *et al.* Orthotopic xenografts of RCC retain histological, immunophenotypic and genetic features of tumours in patients. *J. Pathol.* **225,** 212–221 (2011).
16. Erbay, G. *et al.* Evaluation of malignant and benign renal lesions using diffusion-weighted MRI with multiple b values. *Acta Radiologica* **53,** 359–365 (2012).
17. Larson, P. E. *et al.* Multiband excitation pulses for hyperpolarized 13C dynamic chemical-shift imaging. *J Magn Reson* **194,** 121–127 (2008).
18. Lau, A. Z., Chen, A. P., Hurd, R. E. & Cunningham, C. H. Spectral-spatial excitation for rapid imaging of DNP compounds. *NMR Biomed.* **24,** 988–996 (2011).
19. Larson, P. E. *et al.* Fast dynamic 3D MR spectroscopic imaging with compressed sensing and multiband excitation pulses for hyperpolarized 13C studies. *Magn Reson Med* **65,** 610–619 (2011).
20. Xing, Y., Reed, G. D., Pauly, J. M., Kerr, A. B. & Larson, P. E. Z. Optimal variable flip angle schemes for dynamic acquisition of exchanging hyperpolarized substrates. *Journal of Magnetic Resonance* **234,** 75–81 (2013).